Received: 10 May 2022 | Revised: 24 January 2023 | Accepted: 25 January 2023

DOI: 10.1111/nan.12887

ORIGINAL ARTICLE

Neuropathology and Applied Neurobiology
JOURNAL OF THE BRITISH NEUROPATHOLOGICAL SOCIETY

WILEY

# Regional redistribution of CB1 cannabinoid receptors in human foetal brains with Down's syndrome and their functional modifications in Ts65Dn$^{+/+}$ mice

Ágoston Patthy[1] | János Hanics[1,2] | Gergely Zachar[1] | Gábor G. Kovács[3,4] | Tibor Harkany[5,6] | Alán Alpár[1,2]

[1]Department of Anatomy, Semmelweis University, Budapest, Hungary

[2]SE NAP Research Group of Experimental Neuroanatomy and Developmental Biology, Semmelweis University, Budapest, Hungary

[3]Institute of Neurology, Medical University of Vienna, Vienna, Austria

[4]Department of Laboratory Medicine and Pathobiology and Tanz Centre for Research in Neurodegenerative Disease, University of Toronto, Toronto, Canada

[5]Department of Molecular Neurosciences, Center for Brain Research, Medical University of Vienna, Vienna, Austria

[6]Department of Neuroscience, Biomedicum, Karolinska Institutet, Solna, Sweden

**Correspondence**
Alán Alpár, H-1085 Budapest, Tűzoltó utca 58, Budapest, Hungary.
Email: alpar.alan@med.semmelweis-univ.hu

**Funding information**
This work was supported by the National Brain Research Program of Hungary (2017-1.2.1-NKP-2017-00002 and NAP2022-I-1/2022 to A.A.); the Excellence Program for Higher Education of Hungary (TKP-EGA-25, A.A.); the Swedish Medical Research Council (2018-02838 to T.H.); Novo Nordisk Foundation (NNF20OC0063667 to T.H.); the NKFIH UNKP-22-23 and the FK 131966 grants (to G.Z.); Hjärnfonden (FO2019-0277 to T.H.); and the European Research Council (FOODFORLIFE, 2020-AdG-101021016, and SECRET-DOCK, 2022-PoC2-101082277 to T.H.).

## Abstract

**Aims:** The endocannabinoid system with its type 1 cannabinoid receptor ($CB_1R$) expressed in postmitotic neuroblasts is a critical chemotropic guidance module with its actions cascading across neurogenic commitment, neuronal polarisation and synaptogenesis in vertebrates. Here, we present the systematic analysis of regional $CB_1R$ expression in the developing human brain from gestational week 14 until birth. In parallel, we diagrammed differences in $CB_1R$ development in Down syndrome foetuses and identified altered $CB_1R$ signalling.

**Methods:** Foetal brains with normal development or with Down's syndrome were analysed using standard immunohistochemistry, digitalised light microscopy and image analysis (NanoZoomer). $CB_1R$ function was investigated by in vitro neuropharmacology from neonatal Ts65Dn transgenic mice brains carrying an additional copy of ~90 conserved protein-coding gene orthologues of the human chromosome 21.

**Results:** We detected a meshwork of fine-calibre, often varicose processes between the subventricular and intermediate zones of the cortical plate in the late first trimester, when telencephalic fibre tracts develop. The density of $CB_1Rs$ gradually decreased during the second and third trimesters in the neocortex. In contrast, $CB_1R$ density was maintained, or even increased, in the hippocampus. We found the onset of $CB_1R$ expression being delayed by ≥1 month in age-matched foetal brains with Down's syndrome. In vitro, $CB_1R$ excitation induced excess microtubule stabilisation and, consequently, reduced neurite outgrowth.

**Conclusions:** We suggest that neuroarchitectural impairments in Down's syndrome brains involve the delayed development and errant functions of the endocannabinoid system, with a particular impact on endocannabinoids modulating axonal wiring.

KEYWORDS
cannabinoid receptor, developmental delay, endocannabinoid system, genetic brain disease, neurodevelopmental disorder, trisomy

## INTRODUCTION

The temporal and spatial interaction of chemotropic guidance systems shapes brain development by controlling many aspects of intercellular communication. Amongst these signalling modules, the endocannabinoid system is recognised as one of the most abundant units, which is present in virtually all synapses. Endocannabinoid signalling attracted significant interest recently because of its medical relevance and sensitivity to plant-derived and synthetic drugs [1, 2]. Notably, both the localization and function of the enzymatic machinery controlling endocannabinoid bioavailability and of both the typical and atypical cannabinoid receptors differ between foetal and adult brains [3–6]. Both 2-arachidonoglycerol (2-AG) [7] and anandamide (AEA) [8], the major endocannabinoid ligands, participate in the retrograde control of synaptic plasticity at mature synapses by acting at type 1 cannabinoid receptors ($CB_1Rs$) postnatally [4–6]. In contrast, the endocannabinoid family of small signal lipids serves as one of the guidance systems to define synapse localisation and selection during brain development. Herein, endocannabinoids can act in an autocrine/cell-autonomous fashion when controlling neural progenitor proliferation through non-$CB_1R$-mediated mechanisms [9–12]. Indeed, $CB_1R$ expression is seen as a feature of neurogenic commitment in vertebrates [13], with a marked increase in $CB_1R$ expression and responsiveness once neuroblasts leave their respective progenitor zones [14, 15]. Subsequently, endocannabinoids modulate directional motility for both neurons (cell migration) and their navigating neurites (neuronal polarisation and pathfinding) [16, 17], at least in the cerebral cortex. In doing so, endocannabinoid engagement of $CB_1Rs$ can alter cytoskeletal dynamics in growth cones and neurites [18], alone or in interplay with other signalling systems [19]. Endocannabinoids so far have been suggested to act by volumetric diffusion (although they are released by postsynaptic vesicular exocytosis, in a process that requires synucleins [20]) because signal lipids can likely spread along and within biological membranes. Endocannabinoid signals could thus have a substantial impact, particularly during intrauterine development, when neuronal polarisation and morphogenesis rest on a >1,000-fold expansion of the membrane surface in each neuroblast and when the brain is yet devoid of astroglial and/or oligodendroglial limiting cellular barriers [17]. Despite the incomplete glial map of the antenatal brain, diffusible lipids can instead be spatially confined by recruitment of the enzymatic machinery that controls their availability. For 2-AG, the differential distribution of *sn*-1-diacylglycerol lipases (DAGLα) and monoacylglycerol lipase (MAGL) along growing neurites is one such example to maintain unidirectional lipid signalling [16, 17]. Once the ground plan of the neuronal connectome is complete, endocannabinoid signalling between glia and neurons starts to refine neuronal metabolism and synaptic neurotransmission [19].

Within the family of 'cannabinoid receptors' [21, 22], the $CB_1R$ predominates in the nervous system of both rodents [14] and humans [23]. Because of its abundant expression, neocortical development is thought to rely on $CB_1Rs$-mediated endocannabinoid signalling. Upon synthesis and *trans*-Golgi maturation in neuronal somata [12], $CB_1Rs$ are rapidly transported on small vesicles along corticofugal axons [24].

**Key points**

- This study gives a regional distribution pattern of cannabinoid receptor type 1 expression in the human foetal brain.
- In Down's syndrome, receptor expression is delayed by at least a month.
- $CB_1R$ activation induces excess microtubule stabilisation in cortical neurons of Ts65Dn Down's syndrome model transgenic mice.

The preferential axonal distribution of $CB_1Rs$ can thus steer directional growth decisions [14, 19]. Even before developmental processes are complete, $CB_1Rs$ accumulate in varicose foci in nascent axons, thus marking prospective terminal and/or *en passant* synaptic boutons [25, 26]. This subcellular distribution of $CB_1Rs$ is thus poised to uninterruptedly traverse from growth to the retrograde control of emergent synaptic activity [27, 28]. $CB_1R$ activation during foetal life triggers either mTOR [14, 29] or Erk, PI3K/Akt and c-Jun kinase signalling [30]. For the c-Jun cascade, the rate of c-Jun N-terminal kinase (JNK1) phosphorylation/dephosphorylation represents a major determinant of cytoskeletal instability. This is because JNK1 exerts a direct effect on the availability of SCG10/stathmin-2 by triggering its proteasomal degradation by phosphorylation. SCG10/stathmin-2 itself controls tubulin availability for cytoskeletal reorganisation [18], including during neuritogenesis.

Despite recent progress [31–33], we know little about whether errant endocannabinoid signalling contributes to the pathogenesis of developmental brain disorders or if its changes are instead secondary to the evolving pattern of structural synaptic deficits. The best-known congenital neurological disorders with endocannabinoid involvement are fragile X syndrome [34] and epilepsy [35]. Synaptic impairment in fragile X syndrome, a genetic disorder caused by a mutant form of the *FMR1* gene, is attenuated by non-$CB_1R$-acting cannabidiol (ZYN002) [36]. Alternatively, the efficacy of $CB_1R$ antagonism to reverse synaptic deficits in a mouse model of fragile X syndrome offers a therapeutic perspective [37]. The developmental significance of manipulating endocannabinoid signalling is illustrated by the ability of $CB_1R$ antagonists to shift the excitation/inhibition balance in cortical neurocircuits, thus inducing epileptiform discharges in infants. Conversely, enhanced signalling at $CB_1Rs$ dampens network activity, at least in animal models [25].

Here, we focused on Down's syndrome, or trisomy 21, a major genetic cause of intellectual disability with a probability of about 1-in-700-to-1,000 live births [38]. Epilepsy is a highly prevalent comorbidity of Down's syndrome [39]. At the cellular level, Down's syndrome is characterised by altered cortical lamination and decreased synaptic neurotransmission, the latter being due to the malformation of dendrites, including dendritic spines, which are the structural targets of excitatory synapses [40, 41]. Previously, down-regulation of repressor

element-1 silencing transcription factor (REST)-regulated genes was identified in foetuses with Down's syndrome [42]. Amongst these, *STMN2* (the gene coding the SCG10 protein) was the topmost affected target. This finding is exciting for developmental neurobiologists because it allows us to link SCG10 to upstream $CB_1R$ activity at synapses across the foetal brain [18]. Significantly, SCG10 protein expression in the developing brain is restricted to neuronal contingents that transit from a migratory towards a differentiated/polarised state and are actively engaged in neuritogenesis [43]. Therefore, we first systematically mapped $CB_1R$ distribution in foetal brains with Down's syndrome and age-matched controls. Second, we tested a mechanistic link between $CB_1R$–SCG10 activity-impaired neuritogenesis in foetuses of Ts65Dn$^{+/+}$ mice, which carry an extra copy of a large part of the mouse chromosome 16, resulting in trisomy of around 90 conserved protein-coding gene orthologues to the human chromosome 21 [44–46]. Our findings reveal a temporal mismatch in antenatal $CB_1R$ expression in Down's syndrome vs. age-matched controls, particularly in telencephalic axonal tracts, and implicate excess $CB_1R$-to-SCG10 signalling as a mechanism limiting neuritogenesis.

## MATERIALS AND METHODS

### Neuropathology: Human foetal tissues, their preparation, histochemistry and quantification

To map $CB_1R$ distribution, $n = 13$ male and $n = 14$ female foetal brains with normal development (between gestational weeks 14 and 40) were selected from the Brain Bank of the Institute of Neurology, Medical University of Vienna, Austria. We investigated another $n = 3$ brains for which sex was unknown. Foetal brain tissue was obtained from spontaneous or medically induced abortions. Only cases without genetic disorders, head injury or neurological complications were included as controls. These cases showed neither chromosomal aberrations nor *post-mortem* autolysis. Neuropathological examination excluded major central nervous system malformations, severe hypoxic/ischemic encephalopathy, intraventricular haemorrhage, hydrocephalus, meningitis or ventriculitis. Another $n = 10$ male, $n = 8$ female and $n = 5$ foetal brains with unknown sex but all with Down's syndrome were included in this study. Tissues were obtained and used in compliance with the Declaration of Helsinki and following institutional guidelines. Brain analysis was performed according to an approval for histopathology by the Human Ethical Committee of the Medical University of Vienna (No. 104/2009).

Three-micrometre-thick tissue sections of formalin-fixed, paraffin-embedded tissue blocks were mounted on pre-coated glass slides (StarFrost). Shortly after deparaffinisation and rehydration, the sections were pre-treated in low-pH EnVision FLEX antigen retrieval solution at 98°C for 20 min (PTLink; Dako) and subsequently incubated with a polyclonal anti-$CB_1R$ antibody made in rabbit (gift from Ken Mackie, 1:1,000, [16]). A biotinylated anti-rabbit secondary antibody produced in donkey (K5007, ThermoFisher) and the DAKO EnVision detection kit including peroxidase/3,3-diaminobenzidine-tetrahydrochloride (DAB; Agilent) were used to visualise antibody binding. Immunolabelling of the medulla oblongata, which harbours the corticospinal and corticobulbar tracts known to contain $CB_1Rs$ in mammals [47], served as a positive control to validate the specificity of the anti-$CB_1R^+$ antibody (Figure 1A). Sections were counterstained with haematoxylin, dehydrated in an ascending gradient of ethanol, cleared with xylene and coverslipped with Consil-Mount (Shandon; ThermoFisher) (Figure 1B). Representative images containing the area of interest were automatically captured on a slide-scanner (Nikon) and exported from stored images using the NanoZoomer 2.0 plug-in (Hamamatsu). A semi-quantitative analysis of $CB_1R^+$ varicosities was made with the relative density of these structures classified as 0, +, + +, +++ or ++++. $CB_1R^+$ varicosities were counted in regions of

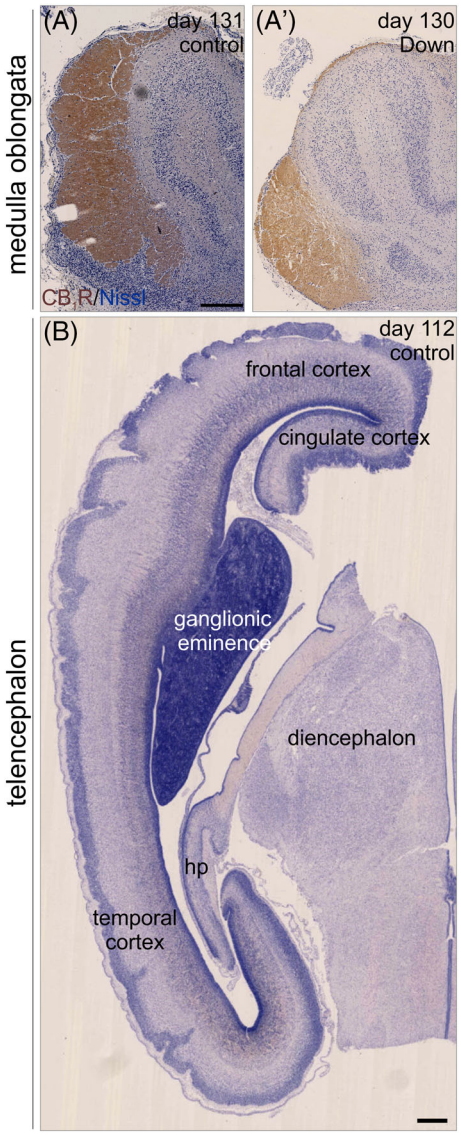


**FIGURE 1** (A, A′) $CB_1R^+$ pyramidal tract axons in the medulla oblongata of control and Down's syndrome subjects. (B) Overview of a foetal forebrain section indicating the regions studied. Abbreviations: $CB_1R$, cannabinoid receptor type 1; ctrl, control; hp, hippocampus. Scale bars = 1 mm

interest and normalised to equivalent surface areas (500 μm$^2$, $n = 10$/area/section) using the NanoZoomer 2.0 toolbox (Figure S1).

For confocal laser scanning microscopy, human samples were deparaffinated, rehydrated, washed in phosphate buffer (0.1 M PB; pH 7.4) and pre-treated with 0.3% Triton X-100 (Sigma; in 0.1 M PB) at 22–24°C for 2 h to enhance antibody penetration [18, 48] (Table S1). To suppress non-specific immunoreactivity, we incubated the tissue specimens in a mixture of 5% (wt/vol) normal donkey serum (NDS; Jackson ImmunoResearch), 2% (wt/vol) BSA (Sigma) and 0.3% Triton X-100 in 0.1 M PB at 22–24°C for another 1.5 h. Sections were then exposed to a mixture of mouse anti-NeuN and rabbit anti-$CB_1R$ antibodies (Table S1) diluted in 0.1 M PB, to which 0.1% NDS and 0.3% Triton X-100 had been added, at 4°C for 16–72 h. Immunoreactivities were revealed by carbocyanine (Cy) 3- or 5-tagged secondary antibodies raised in donkey (1:200; Jackson) and applied at 22–24°C for 2 h. Nuclei were counterstained with Hoechst 33,421 (1:10,000; Sigma). Sections were dehydrated in an ascending gradient of ethanol, cleared with xylene and coverslipped with DePeX (ACM, Fluka). Images were captured on an LSM780 confocal laser-scanning microscope (Zeiss) with optical zoom ranging from 1–3X when using a 40X (Plan-Apochromat 40X/1.40) objective and the pinhole set to 0.5–0.7 μm ('optical thickness').

## Experimental neurobiology: Dissociated cortical cultures of neonatal mice

On postnatal day 2 (P2), whole neocortices were dissected out from wild-type and littermate Ts65Dn$^{+/+}$ mice, the most common model of Down's syndrome [44–46]. Tissues were enzymatically dissociated and plated at a density of 200,000 cells/well in six-well plates for Western blotting. On day 2 in vitro (DIV), neurons were stimulated by WIN55,212-2 (500 nM, Tocris) for 30 min (control cultures received no vehicle treatment; we did not include WIN55,212-3 either because our earlier studies did not reveal any drug effect at 500 nM [49]) and lyzed immediately afterwards (see below).

Alternatively, primary neurons were seeded at a density of 50,000 cells/well on poly-D-lysine-coated coverslips in 24-well plates and maintained in DMEM/F12 (1:1) containing B27 supplement [2% (vol/-vol)], L-glutamine (2mM), penicillin (100 U/ml) and streptomycin (100 μg/ml) (all from Invitrogen). Neurons were challenged with WIN55,212-2 (500 nM) for 30 min on DIV2 and kept alive for another 24 h in maintenance medium (DMEM/F12/B27). Subsequently, cells on coverslips were immersion-fixed in ice-cold 4% paraformaldehyde in 0.05 M PB for morphometry. The rationale of this experiment was to test if Ts650Dn$^{+/+}$ neurons could overcome WIN55,212-2-induced growth arrest, as is known for wild-type neurons [18, 24, 49].

## Western blotting

Neurons were collected and homogenised by sonication in TNE buffer containing 0.5% Triton X-100 (Sigma), 1% octyl-β-D-glucopyranoside (Calbiochem), 5mM NaF, 100 μM $Na_3VO_4$ and a mixture of protease inhibitors (Complete™; Roche). Cell debris and nuclei were pelleted by centrifugation (800×$g$ at 4°C for 10 min). Protein concentration was determined by Bradford's colourimetric method [50]. Samples were diluted to a final protein concentration of 2 μg/μl, denatured in 5× Laemmli buffer and analysed by SDS-PAGE on 8% or 10% (vol/-vol) resolving gels. After transfer onto Immobilon-FL PVDF membranes (Millipore), membrane-bound protein samples were blocked in 3% (wt/vol) BSA and 0.5% Tween-20 diluted in TRIS-buffered saline (for 1.5 h) and exposed to primary antibodies (Table S1) at 4°C overnight. Appropriate combinations of horseradish peroxidase (HRP)-conjugated secondary antibodies from goat, rabbit or mouse hosts (Jackson; 1:10,000; 2 h) were used for signal detection. Image acquisition and analysis were performed on a Bio-Rad XRS$^+$ imaging platform.

## Immunocytochemistry

Coverslips were rinsed in 0.1 M PB (pH 7.4) and pre-treated with 0.3% Triton X-100 (Sigma; in PB) at 22–24°C for 1 h to enhance the penetration of primary antibodies [18, 48] (Table S1). Non-specific immunoreactivity was suppressed by incubating our specimens in a mixture of 5% (wt/vol) NDS (Jackson), 2% (wt/vol) BSA (Sigma) and 0.3% Triton X-100 in 0.1 M PB at 22–24°C for another 1 h. Coverslips were then exposed to mouse anti-β-III-tubulin and rabbit anti-SCG10 primary antibodies (Table S1) diluted in 0.1 M PB, to which 0.1% NDS and 0.3% Triton X-100 had been added, at 4°C for 16–72 h. Immunoreactivities were revealed by carbocyanine (Cy) 2- or 3-tagged secondary antibodies raised in donkey (1:200; Jackson) and applied at 22–24°C for 2 h. Nuclei were routinely counterstained by Hoechst 33,421 (1:10,000; Sigma). Coverslips were drop-dried and mounted onto fluorescence-free glass slides with glycerol/gelatin (GG-1; Sigma). Images were captured on an LSM780 confocal laser-scanning microscope (Zeiss) with optical zoom ranging from 1–3X when using a 40X (Plan-Apochromat 40X/1.40) objective and the pinhole set to 0.5–0.7 μm ('optical thickness'). Emission spectra for the dyes were limited to 450–480 nm (Hoechst 33,421), 505–530 nm (Cy2) and 560–610 nm (Cy3).

## Statistics

Data were expressed as means ± s.e.m. Morphological parameters were statistically compared between control ($n = 3$) and Down's syndrome ($n = 3$) subjects in equivalent age groups using two-tailed, paired Student's $t$ tests with gestational age being the intrinsic variable for pairing (GraphPad Prism). A two-tailed Student's $t$ test for independent samples was used to test pharmacological and genetic variables in vitro. A $p$ value of <0.05 was taken as indicative of statistical differences. Multi-panel figures were assembled in CorelDraw X7 (Corel Corp.). The cohort available allowed us to investigate sex-specific differences only between gestational days 121–160. Applying

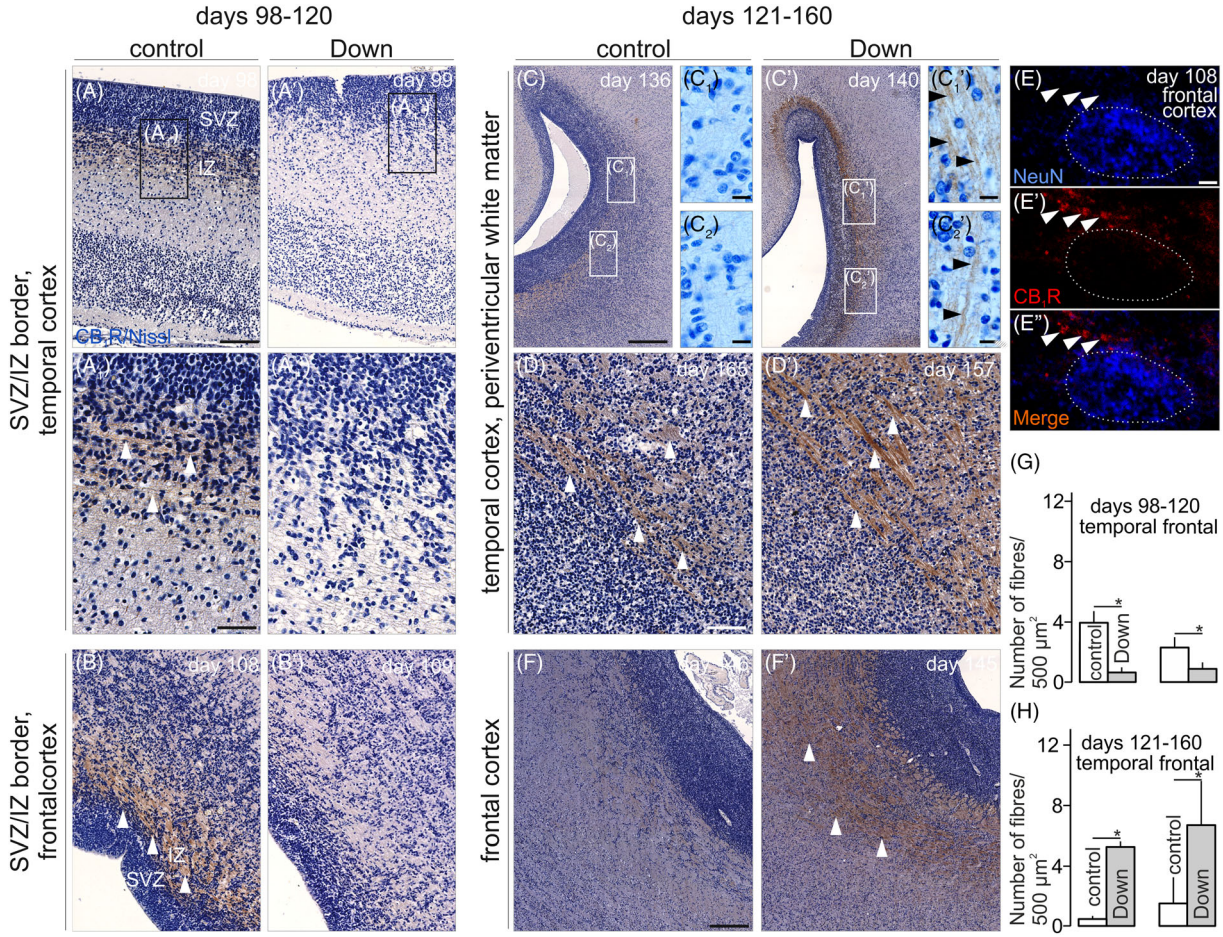


**FIGURE 2** Axonal $CB_1Rs$ in the neocortex in Down syndrome. Panels A-B′ and C-E′ show specimens between days 98–120 and 121–160, respectively. (A–$A_1$′) $CB_1R^+$ fibres in the SVZ/IZ zone of the temporal cortex in control but not in Down's syndrome subjects (*arrowheads* point to $CB_1R^+$ axons). (B, B′) $CB_1R^+$ fibres in the SVZ/IZ zone of the frontal cortex in control but not in Down syndrome subjects (*arrowheads*). (C–D′) Between days 121 and 160, $CB_1R^+$ processes dominated in Down's syndrome vs. control subjects in the periventricular temporal cortex (*white arrowheads* in D and D′). (E–E″) Extrasomatic $CB_1R^+$ profiles (*white arrowheads*). (F, F′) $CB_1R^+$ axonal bundles in Down's syndrome but not in control brains (*white arrowheads* in F′). (G) The density of $CB_1R^+$ fibres was lower in temporal and frontal cortices of subjects with Down's syndrome between days 98 and 120, as compared to age-matched controls. (H) $CB_1R^+$ density of subjects with Down's syndrome exceeded that of control subjects in the temporal and in frontal cortex between days 121 and 160. Abbreviations: $CB_1R$, cannabinoid receptor type 1; ctrl, control. Scale bar = 1 mm (C, F), 300 µm (A, D), 100 µm ($A_1$) and 3 µm ($C_1$)

the five unit scales (0, +, ++, +++, ++++; see first paragraph of this section), we used ordinal logistic regression models to investigate the interaction between Down's syndrome status and sex.

## RESULTS

### Neuropathology

$CB_1R^+$ processes and varicosities appeared as fine-calibre meshworks in most brain areas. Here, we first determined their distribution in cortical areas, hippocampal subfields and the cerebellum across the three trimesters of pregnancy. Our principal finding is the delayed appearance and persistent maintenance of $CB_1R^+$ fibres in foetuses with Down's syndrome as late as the fourth month of pregnancy, which contrasts the early and transient presence of $CB_1R^+$ axons coincident with their active growth processes in control foetuses.

### Disrupted temporal dynamics of $CB_1R$ expression in Down's syndrome in the second trimester

In control subjects, a dense bundle of $CB_1R^+$ fibres at the boundary between the cortical subventricular (SVZ) and intermediate zones (IZ) was detected, being particularly notable in the temporal cortex, between days 98 and 120 (Figure 2A, $A_1$). In contrast, less and weakly immunoreactive fibres were only visible in age-matched Down's syndrome samples in the corresponding regions (Figure 2A′, $A_1$′, G; Table 1). We came across similar differences when assessing the frontal cortex at the same intrauterine age (Figure 2B, B′, G; Table 1).

**TABLE 1** Semi-quantitative analysis of $CB_1R$-expressing fibres in the subventricular and intermediate zones of the developing neocortex in human foetuses

| Control subjects | | | Down syndrome subjects | | |
|---|---|---|---|---|---|
| **Slide No. and age** | **Temporal cortex** | **Frontal cortex** | **Slide No. and age** | **Temporal cortex** | **Frontal cortex** |
| **Days 98–120** | | | | | |
| 4-12-2 day 98, f | ++ | + | 169-09-2 day 99, nn | 0 | 0 |
| 240-11-2 day 98, m | ++ | + | 156-11-3 day 102, nn | Not on slide | 0 |
| 56-11-2 day 105, f | Not on slide | + | 73-11-2 day 109, nn | 0 | + |
| 33-11-3 day 106, f | Not on slide | ++ | 67-09-2 day 111, f | Not on slide | 0 |
| 178-10-1 day 108, nn | +++ | +++ | 194-09-2 day 112, nn | 0 | 0 |
| 104-11-2 day 119, nn | ++ | 0 | 194-09-3 day 112, nn | 0 | 0 |
| | | | 113-06-2 day 112, m | Not on slide | 0 |
| | | | 50-05-2 day 116, f | 0 | + |
| | | | 171-07-1 day 119, f | 0 | Not on slide |
| **Days 121–160** | | | | | |
| 131-11-2 day 125, f | Not on slide | 0 | 228-07-3 day 128, f | 0 | + |
| 131-11-3 day 125, f | + | + | 66-09-2 day 130, f | 0 | 0 |
| 29-12-1 day 131, m | Not on slide | ++ | 4-09-2 day 131, m | Not on slide | ++ |
| 74-11-2 day 133, nn | 0 | + | 4-09-4 day 131, m | + | +/++ |
| 151-11-2 day 136, m | 0 | 0 | 90-08-2 day 135, f | ++ | + |
| 151-11-3 day 136, m | ++ | +++ | 147-05-2 day 138, m | Not on slide | + |
| 184-10-2 day 137, m | 0 | 0 | 95-10-1 day 140, m | +++ | +++ |
| 39-11-2 day 137, f | 0 | 0 | 118-07-1 I day 145, m | + | + |
| 192-11-2 day 146, m | 0 | + | 118-07-1 II day 145, m | 0 | ++++ |
| 149-10-2 day 148, f | 0 | + | 41-11-2 day 151, m | ++++ | ++++ |
| 236-11-2 day 149, m | + | 0 | 224-11-2 day 155, f | 0 | 0 |
| 127-11-2 day 154, m | 0 | Not on slide | 36-11-3 day 156, m | + | 0 |
| 216-11-2 day 158, m | 0 | 0 | 119-04-2 I day 157, m | ++ | + |
| 128-11-2 day 159, m | 0 | Not on slide | 119-04-2 II day 157, m | +++ | +++ |
| **Days 173–240** | | | | | |
| 207-10-1 day 182, m | 0 | 0 | 47-02-1 day 173, f | 0 | 0 |
| 216-09-4 day 194, m | 0 | 0 | 239-08-4 day 231, m | 0 | Not on slide |
| 72-09-3 day 197, f | 0 | 0 | 53-01-1 day 235, m | 0 | Not on slide |
| 54-10-2 day 235, f | 0 | 0 | 53-01-2 day 235, m | Not on slide | 0 |
| 40-11-2 day 242, f | 0 | 0 | 229-08-1 day 236, m | Not on slide | 0 |
| 40-11-3 day 242, f | 0 | Not on slide | 229-08-2a day236, m | 0 | 0 |
| | | | 229-08-2b day 236, m | 0 | 0 |

Cortical differences appeared throughout the areas irrespective of their 'phylogenetic age': Although axons and dendrites were difficult to distinguish, allocortical hippocampi were also rich in fine $CB_1R^+$ immunoreactive fibres in control subjects during the fourth month of gestation, which contrasted those in Down's syndrome (Figure 3A–$A_1'$; Table 2). Likewise, processes coursing in the fornix, which likely correspond to hippocampal efferent axons emanating from the subiculum, were $CB_1R^+$ in control but not in Down's syndrome cases (Figure 3A, A′). Conversely, $CB_1R^+$ axons invaded the cingulate gyrus (even its dorsal part) in Down's syndrome but not in control foetuses (Figure 3B, B′,E).

Between gestational days 121–160, $CB_1Rs$ were redistributed with remarkable alterations in Down's syndrome foetuses: In the temporal cortex, $CB_1R^+$ processes first appeared adjacent to the cortical proliferative zone (at the SVZ/IZ boundary) around day 140. This contrasted the weakening expression of $CB_1Rs$ in controls (Figure 2C,C′; Table 1). At this stage, we identified $CB_1R^+$ fibres at a higher density in Down's syndrome and considered them as ectopic and likely transient, relative to controls (Figure 2$C_1$–$C'_2$,H; Table 1). $CB_1R^+$ immunoreactivity of periventricular processes in Down's syndrome remained greater than those in age-matched controls, at least until day 160 (Figure 2D,D′; Table 2). $CB_1R^+$ processes

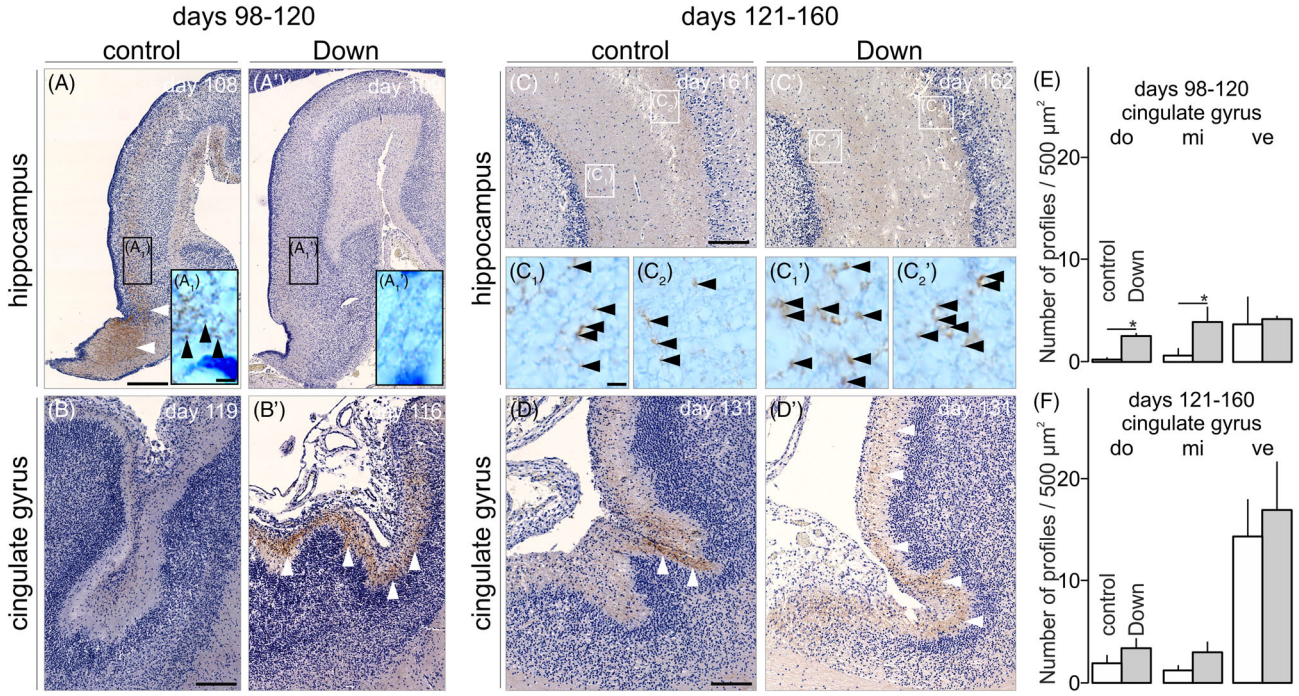


**FIGURE 3** Axonal $CB_1Rs$ in the hippocampus in Down's syndrome. Panels A–B′ and C–E' show specimens between days 98–120 and 121–160, respectively. (A–$A_1$′) In control subjects, hippocampal $CB_1R^+$ fibres appear in the Ammon's horn (*black arrowheads* in $A_1$) and in the fornix (*white arrowheads* in A). Poor immunolabelling was noted in Down's syndrome subjects. (B, B′) In the cingulate gyrus, $CB_1R^+$ fibres appeared in Down's syndrome (*white arrowheads* in E′) but not in control subjects. (C–$C_2$′) Thin $CB_1R^+$ fibres and varicosities in both the lacunosomolecular and the pyramidal layers of the hippocampus (*black arrowheads* in $C_1$, $C_2$, $C_1$′ and $C_2$′ point to immunoreactive terminals). (D, D′) $CB_1R^+$ fibres invaded the dorsal part of the cingulate gyrus in Down's syndrome but not control foetal brains (*white arrowheads* point to immunoreactive fibres). (E) In the ventral and middle parts of the cingulate gyrus, $CB_1R^+$ fibre density was higher in Down's syndrome relative to control between days 98 and 120. (F) No significant difference appeared in any of the investigated parts of the cingulate gyrus in Down's syndrome vs. control subjects between days 121 and 160. Abbreviations: $CB_1R$, cannabinoid receptor type 1; ctrl, control. Scale bars = 1 mm (A–C); 3 µm ($A_1$, $C_1$)

often carried pearl-lace-like swellings, which we considered as nascent varicosities instead of mature synapses. We did not detect $CB_1R$ immunoreactivity overlapping with NeuN; instead, we typically observed $CB_1R^+$ varicosities amongst or around $NeuN^+$ perikarya (Figure 2E–E″), supporting their axonal identity. $CB_1R$ expression and distribution in the frontal cortex did not differ from those in temporal areas (Figure 2F,F′,H; Table 1). In the control hippocampi, $CB_1R^+$ varicose structures were first seen in the Ammon's horn around day 160 (Figure 3C,$C_1$,$C_2$; Table 2) and occurred more often in all developing suprapyramidal layers, including the strata radiatum and lacunosomoleculare, in Down's syndrome cases (Figure 3C,$C_1$′, $C_2$′; Table 2). In the cingulate gyrus of control samples, $CB_1R^+$ fibres were first detected by day 130. However, the immunoreactivity in the equivalent structure of Down's syndrome cases had again greater labelling (Figure 3D,D′,F).

The sex of the embryos had no significant effect on the $CB_1R^+$ label intensity either in neocortex or in allocortex (temporal cortex: W = 2.05, $p$ = 0.153; frontal cortex: W = 2.81, $p$ = 0.094; fimbriae/fornix: $W_{3,149}$ = 0.002, $p$ = 0.962; pyramidal layer of the hippocampus: W = 2.36, $p$ = 0.127; molecular layer of the hippocampus: W = 0.435, $p$ = 0.509; dentate gyrus: W = 0.83, $p$ = 0.362).

## Differences in $CB_1R$ expression during the 3rd trimester

Next, we focused on differences between Down's syndrome and age-matched control subjects during the last trimester of pregnancy. $CB_1R^+$ processes were not detected in the temporal and frontal cortices of either control or Down's syndrome subjects (Figure 4A–$B_1$′; Table 1). Instead, $CB_1R$ immunoreactivity appeared in the prospective layer V of the cingulate gyrus, but without a disease-related difference (Figure 4C–$C_1$′). In the hippocampus, $CB_1R^+$ profiles populated all subfields of the hippocampal formation (Table 2), including the strata pyramidale and moleculare of the Ammon's horn (Figure 4D–$D_2$′), at equivalent densities between Down's syndrome and age-matched cases (Table 2). Likewise, $CB_1R^+$ profiles decorated the indusium griseum, the anterior extension of the hippocampal formation [51], of both control and Down's syndrome subjects (Figure 4F–$F_1$′).

A notable difference was found in the cerebellar cortex; its molecular layer contained a meshwork of fine-calibre $CB_1R^+$ processes in Down's syndrome but not in control brains around day 240 (Figure 4E,E′), a difference that existed since gestational days 130–140 (data not shown).

**TABLE 2** Semi-quantitative analysis of $CB_1R$-expressing fibres in the hippocampal formation of human foetuses

| Control subjects | | | | | Down syndrome subjects | | | | |
|---|---|---|---|---|---|---|---|---|---|
| **Slide No. and age** | **Fim/for** | **Pyr** | **Mol** | **Dent** | **Slide No. and age** | **Fim/for** | **Pyr** | **Mol** | **Dent** |
| **Days 98–120** | | | | | | | | | |
| 4-12-2 day 98, f | +++ | + | 0 | Not on slide | 169-09-2 day 99, nn | 0 | 0 | Not on slide | Not on slide |
| 240-11-2 day 101, m | ++ | 0 | 0 | 0 | 156-11-3 day 102, nn | 0 | Not on slide | Not on slide | Not on slide |
| 56-11-2 day 105, f | +++ | Not on slide | Not on slide | Not on slide | 73-11-2 day 109, nn | + | 0 | + | 0 |
| 33-11-3 day 106, f | +/++ | Not on slide | Not on slide | Not on slide | 194-09-2 day 112, nn | + | 0 | + | 0 |
| 178-10-1 day 108, nn | +++ | + | +++ | + | 194-09-3 day 112, nn | 0 | 0 | + | 0 |
| 104-11-2 day 119, nn | + | + | ++ | + | 113-06-2 day 112, m | 0 | Not on slide | Not on slide | Not on slide |
| | | | | | 50-05-2 day 116, f | +++ | + | +++ | + |
| | | | | | 171-07-1 day 119, f | 0 | 0 | + | 0 |
| **Days 121–160** | | | | | | | | | |
| 131-11-2 day125, f | 0 | Not on slide | Not on slide | Not on slide | 61-12-1 day 126, m | 0 | + | ++ | + |
| 131-11-3 day 125, f | 0 | + | ++ | + | 228-07-3 day 128, f | + | Not on slide | Not on slide | Not on slide |
| 29-12-1 day 131, m | 0 | Not on slide | Not on slide | Not on slide | 66-09-2 day 130, f | 0 | 0 | ++ | 0 |
| 74-11-2 day 133, nn | 0 | + | ++ | + | 4-09-2 day 131, m | + | Not on slide | Not on slide | Not on slide |
| 151-11-2 day 136, m | 0 | 0 | ++ | + | 4-09-4 day 131, m | ++ | + | +++ | + |
| 151-11-3 day 136, m | +++ | ++ | ++++ | +++ | 90-08-2 day 135, f | + | + | + | 0 |
| 39-11-2 day 137, f | + | ++ | +++ | ++ | 147-05-2 day 138, m | + | Not on slide | Not on slide | Not on slide |
| 192-11-2 day 146, m | + | + | ++ | ++ | 95-10-1 day 140, m | ++ | ++ | +++ | ++ |
| 149-10-2 day 148, f | ++ | ++ | +++ | +++ | 118-07-1 I day 145, m | + | ++ | +++ | ++ |
| 236-11-2 day 149, m | 0 | + | ++ | ++ | 118-07-1 II day 145, m | +++ | + | ++ | + |
| 127-11-2 day 154, m | 0 | Not on slide | Not on slide | Not on slide | 41-11-2 day 151, m | ++++ | +++ | ++++ | ++++ |
| 216-11-2 day 158, m | + | 0 | + | + | 224-11-2 day 155, f | 0 | ++ | ++/+++ | ++ |
| 128-11-2 day 159, m | 0 | Not on slide | Not on slide | Not on slide | 36-11-3 day 156, m | 0 | + | ++ | + |
| | | | | | 119-04-2 I day 157, m | +++ | +++ | ++++ | ++++ |
| | | | | | 119-04-2 II day 157, m | +++ | +++ | ++++ | ++++ |
| | | | | | 60-05-2 day 158, m | 0 | + | ++ | Not on slide |

(Continues)

**TABLE 2** (Continued)

| Control subjects | | | | | Down syndrome subjects | | | | |
|---|---|---|---|---|---|---|---|---|---|
| **Slide No. and age** | **Fim/for** | **Pyr** | **Mol** | **Dent** | **Slide No. and age** | **Fim/for** | **Pyr** | **Mol** | **Dent** |
| **Days 173–240** | | | | | | | | | |
| 207-10-1 day 182, m | + | +/++ | ++ | Not on slide | 47-02-1 day 173, f | + | ++ | +++ | ++ |
| 216-09-4 day 194, m | 0 | + | + | + | 239-08-4 day 231, m | 0 | ++++ | +++ | ++++ |
| 72-09-3 day 197, f | + | +++ | +++ | +++ | 53-01-1 day 235, m | 0 | +++ | ++ | +++ |
| 54-10-2 day 235, f | 0 | + | +++ | Not on slide | 229-08-1 day 236, m | 0 | Not on slide | Not on slide | Not on slide |
| 40-11-2 day 242, f | 0 | ++++ | ++++ | ++++ | 229-08-2a day 236, m | 0 | ++++ | +++ | ++++ |
| 40-11-3 day 242, f | 0 | ++++ | +++ | ++++ | 229-08-2b day 236, m | 0 | ++++ | +++ | ++++ |

In sum, our data on human neurodevelopment suggest that $CB_1R$ expression marks delayed axonal development in Down's syndrome, which is mostly overcome by the third trimester when synaptogenesis dominates. Nevertheless, the impaired positioning of $CB_1Rs$ during mid-gestation could imprint long-lasting modifications on neuronal structure and function, thus adversely impacting synaptic plasticity in affected offspring. To experimentally test this hypothesis, we resorted to $CB_1R$ pharmacology in Ts65Dn$^{+/+}$ mice (vs. littermate controls), which represent a tractable genetic model of Down's syndrome [45].

## $CB_1R$ stimulation induces SCG10 degradation and tubulin ageing in Ts65Dn$^{+/+}$ neurons

$CB_1R$ stimulation impairs neuritogenesis by inducing an Erk/Jnk1-dependent SCG10 degradation pathway, which coincidentally increases the presence of acetylated tubulin in shortened neurites [18]. This is because SCG10 binds tubulin dimers in a $CB_1R$-dependent fashion [43] and its degradation increases microtubule stability (termed 'ageing') [18]. Here, we tested the hypothesis that Ts65Dn$^{+/+}$ neurons could have differential responses to agonist stimulation of $CB_1Rs$, particularly since many duplicated genes in this mouse model affect kinase signalling and protein degradation.

SCG10 accumulated in the perikarya of cultured neurons, with a selective concentration in axonal varicosities, as well as the growth cone in both Ts65Dn$^{+/+}$ and wild-type neurons (Figure 5A′–$A_2$,B–$B_2$). SCG10$^{+}$ neurite segments were more proximal to the somata on the Ts65Dn$^{+/+}$ background, as compared to wild-type neurons (Figure 5E; 76.41 ± 3.59% [Ts65Dn] vs. 85.5 ± 2.2% [wild-type], as of total neurite length, $p = 0.02$), confirming differential protein localization under non-stimulated conditions. When exposing neurons to WIN55,212-2 (500 nM) for 30 min [18], we found Ts65Dn$^{+/+}$ neurons to show excess SCG10 degradation, particularly in their distal (motile) neurite segments (Figure 5C′–$C_2$,D–$D_2$,E; 52.46 ± 3.85% [Ts65Dn] vs. 90.29 ± 3.1% [wild-type], of total neurite length, $p < 0.01$). Moreover, WIN55,212-2 decreased the relative intensity of distal-most SCG10 immunoreactivity in neurites (as compared to somatic SCG10 intensity) in Ts65Dn$^{+/+}$ (12.78 ± 2.8% [WIN55,212–2] vs. 53.55 ± 7.03% [no treatment], scaled intensity values, $p < 0.01$) but not in wild-type neurons (Figure 5F; 59.75 ± 11.35% [WIN55,212-2] vs. 43.06 ± 5.16% [no treatment], $p = 0.13$). The increased accumulation of acetylated tubulin is often used as a surrogate of excess SCG10 degradation [52]. Indeed, WIN55,212-2 treatment increased tubulin acetylation in Ts65Dn$^{+/+}$ but not control neurons (Figure 5H,H′). Thus, our data suggest neuronal hypersensitivity to $CB_1R$'s stimulation in Ts65Dn$^{+/+}$ mice, whose developmental consequence is slowed neuritogenesis.

## Neurons from Ts65Dn mice exhibit slowed $CB_1R$-dependent neuritogenesis in vitro

The general physiological paradigm for $CB_1R$-mediated growth responses is that $CB_1R$ stimulation stalls neurite growth in primary cells [53, 54], which can be overcome if agonist stimulation of the $CB_1Rs$ is only brief. The differential expression and distribution of $CB_1Rs$ in Down's syndrome together with the increased sensitivity of the SCG10 pathway to $CB_1R$ stimulation in Ts65Dn$^{+/+}$ mice suggest that disrupted $CB_1R$ functionality, rather than altered localization, could underscore slowed neurite growth. Therefore, and relying on our SCG10 data (see above), we challenged Ts65Dn-derived and wild-type cortical neurons with WIN55,212-2 for 30 min and allowed them to grow for another day. Under control conditions, Ts65Dn$^{+/+}$ neurons grew significantly slower than their wild-type counterparts in vitro (Figure 5A–$B_2$,G; 54.74 ± 3.56 μm [Ts65Dn] vs. 69.16 ± 4.33 μm [wild-type], $p = 0.02$). Notably, wild-type neurons had slightly, albeit non-significantly, longer neurites on DIV3 (Figure 5G), which we interpreted as relative resistance to the low-dose WIN55,212-2 exposure (30 min). In contrast, WIN55,212-2 occluded neurite outgrowth in Ts65Dn$^{+/+}$ neurons (Figure 5C–$D_2$,G; 46.3 ± 4.17 μm [Ts65Dn] vs. 82.62 ± 6.66 μm [wild-type], $p < 0.01$). These data suggest that neuritogenesis is per se slowed in Ts65Dn$^{+/+}$

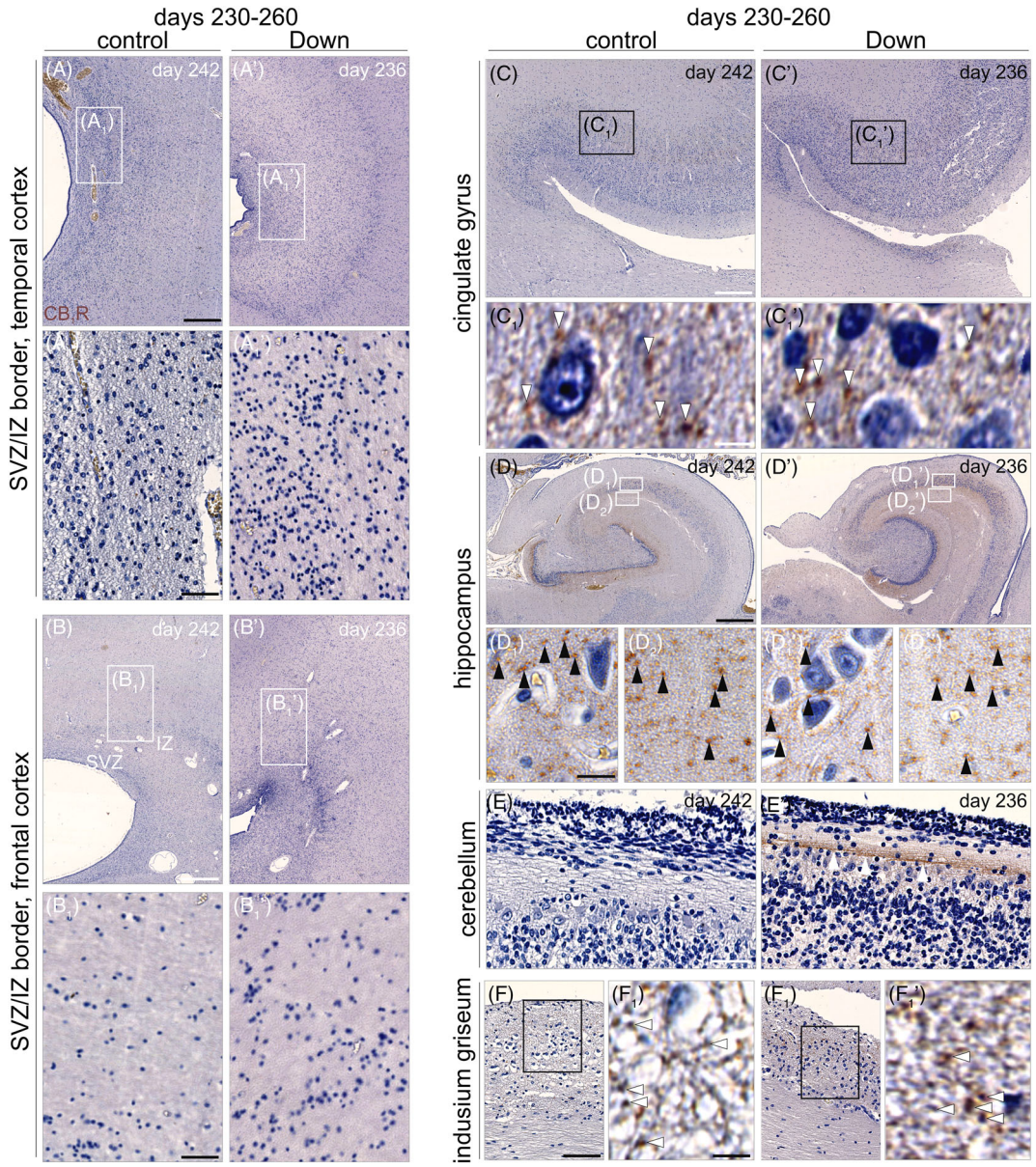


**FIGURE 4** $CB_1R$ expression in control and Down's syndrome subjects during the 3rd trimester. (A–$A_1$′) $CB_1Rs$ were absent at the SVZ/IZ boundary in the temporal cortex of both control and Down's syndrome cases. (B–$B_1$′) Similarly, $CB_1R^+$ processes did not appear in the frontal cortex either. (C–$C_1$′) $CB_1R^+$ structures (*white arrowheads* in $C_1$, $C_1$′) in the inner pyramidal layer of the cingulate gyrus. (D–$D_2$′) $CB_1R^+$ profiles in the strata pyramidale (*black arrowheads* in $D_1$, $D_1$′) and radiatum (*black arrowheads* in $D_2$, $D_2$′) of Ammon's horn. (E, E′) $CB_1R^+$ processes were present in the cerebellar molecular layer in Down's syndrome (*white arrowheads* in E′) but not in control subjects. (F–$F_1$′) $CB_1R^+$ structures in the indusium griseum. Abbreviations: $CB_1R$, cannabinoid receptor type; ctrl, control; IZ, intermediate zone; SVZ, subventricular zone. Scale bars = 1 mm (A–D), 300 μm (F); 100 μm ($A_1$, $B_1$, E); 5 μm ($C_1$, $D_1$, $F_1$)

neurons and coincides with enhanced sensitivity to agonist-induced $CB_1R$ signalling.

## DISCUSSION

Previous studies reported *CNR1*/$CB_1R$ mRNA expression in limbic cortices of the human foetal brains from mid-gestation (weeks 18-22) [55] and proposed vulnerability to exogenous cannabinoids [2]. Autoradiography of foetal brains (19–40 weeks of gestation) demonstrated that $CB_1Rs$ are functional and their expression increases progressively until adulthood [56]. Here, we provide a regional survey of $CB_1R$-expressing neurites at the light microscopy level spanning the period of the late first trimester (week 14) until birth. We demonstrate that the regional distribution of $CB_1Rs$ follows area-specific temporal scales. Our study employed high-resolution light-and confocal laser scanning microscopy. Unfortunately, the often lengthy *post-mortem* delay and the conditions of

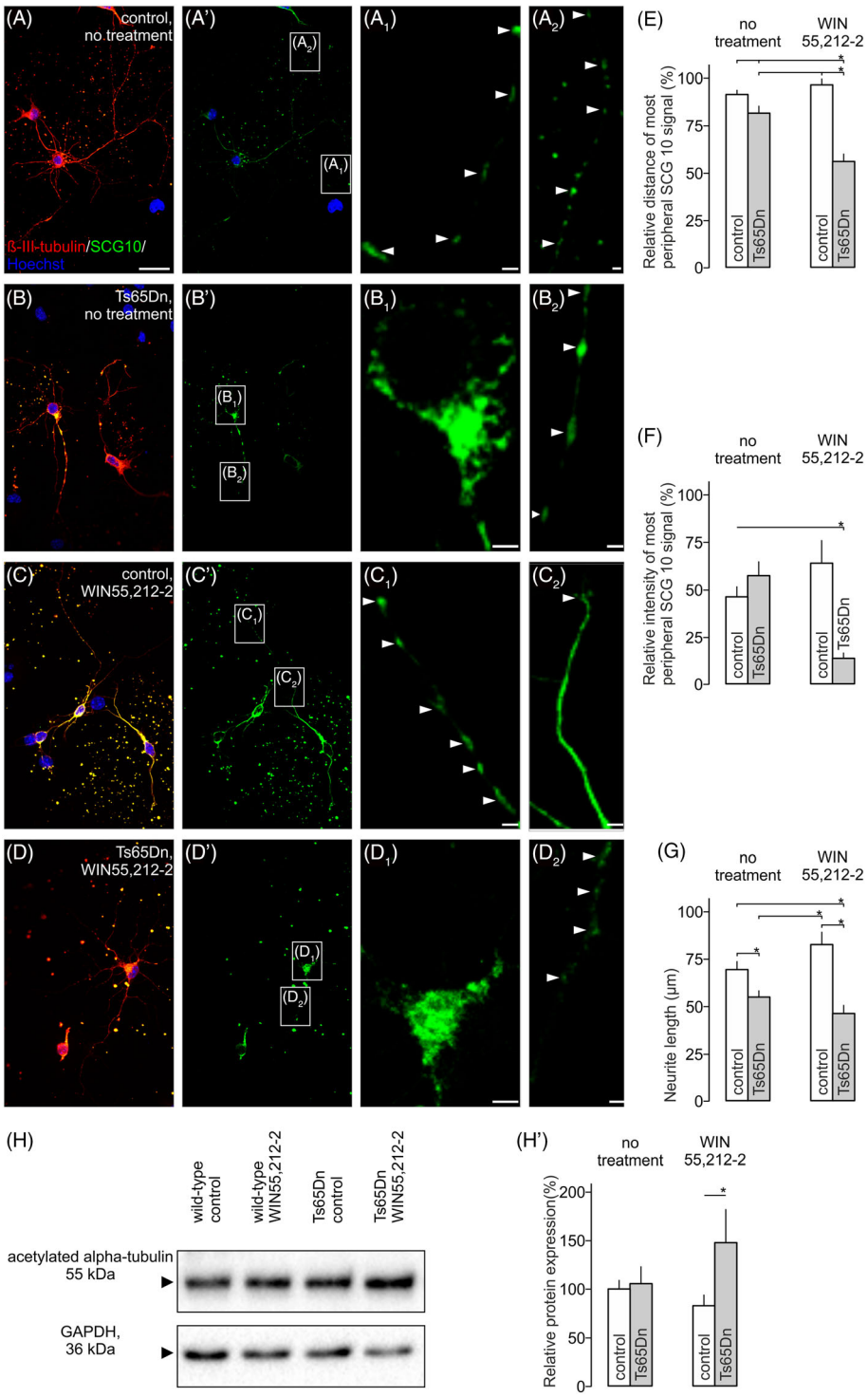


**FIGURE 5** Neurons from Ts65Dn$^{+/+}$ mice develop shorter neurites in a $CB_1R$-dependent fashion in vitro. (A–$A_2$) Neocortical neurons of control littermate mice. Primary neuronal culture on P2. Arrowheads indicate SCG 10-immunoreactivity in a neurite. (B–$B_2$) Neocortical neurons of Ts65Dn$^{+/+}$ mice. Primary neuronal culture on P2. Note the somatic accumulation of SCG10 in $B_1$. Arrowheads in $B_2$ indicate SCG10 immunoreactivity in a neurite. (C–$C_2$) WIN55,212-2 increased SCG10 expression (*arrowheads* in $C_1$; arrowhead in $C_2$ points to neurite end) in control cultures. (D–$D_2$) WIN55,212-2 in primary neuronal cultures from Ts65Dn$^{+/+}$ mice reduced SCG10 immunoreactivity in neurites (*arrowheads*). (E) WIN55,212-2 reduced the distance of peripheral SCG10 immunoreactivity. (F) WIN55,212-2 reduced the intensity of peripheral SCG10 immunosignal. (G) Neurons isolated from Ts65Dn$^{+/+}$ mice and cultured in vitro had shorter neurites. (H, H′) WIN55,212-2 increased the expression of acetylated tubulin in neurons from Ts65Dn$^{+/+}$ but not wild-type littermate mice. Abbreviation: ctrl, control. Scale bars = 20 µm (A); 3 µm ($B_1$, $D_1$); 2 µm ($A_1$, $A_2$, $B_2$, $C_2$, $D_2$)

tissue preservation did not allow for ultrastructural analysis. Therefore, we have not drawn conclusions on, e.g., the subcellular compartmentalization of $CB_1Rs$, and the number, level of structural maturation, neurochemical identity or the ability of vesicular exocytosis of putative $CB_1R^+$ synapses. Instead, we referred to 'varicosities', a morphological descriptor purely considering the shape of $CB_1R^+$ structures. Nevertheless, ultrastructural data from the rodent and primate neocortex revealed $CB_1R$ expression in the somata of neurons radially migrating across the cortical plate [12]. The expression of $CB_1R$ at the early neuroblast phase is relevant to (endo-)cannabinoid-induced nucleokinesis [57], a key step of directional chemotaxis. While we can neither confirm nor exclude the somatic localization and presence of $CB_1R$-containing intracellular vesicles in the cortex of human foetuses, our imaging data support the conclusion that disproportionately many $CB_1Rs$ reside in neurites to efficiently modulate neuritogenesis.

In contrast to the adult pattern, long-range projection neurons (e.g., cortical pyramidal cells) are the primary source of $CB_1Rs$ in the developing forebrain [14, 58], a finding that corroborates model studies showing that pathfinding decisions and fasciculation steps also rely on $CB_1R$-mediated signalling events [18, 24, 59]. Due to their vast number and diverse subtypes (including associative, commissural and projection), $CB_1R^+$ axons were visualised throughout the developing human foetal forebrain. The immunoreactive processes, which were typically positioned as if they were white matter pathways, harboured $CB_1R^+$ varicosities. Varicose structures were numerous at the SVZ–IZ boundary of all telencephalic areas [60], including both the neocortex and allocortex.

Down's syndrome is characterised by reduced neurogenesis [61, 62], an imbalance of the projection neuron/interneuron ratio, and astrogliosis [63]. The reduced number of dendritic spines and synaptosomal structures reflect defunct morphogenesis [64]. Most of these observations are based on results described in foetal brains from the second trimester. Likely, these changes shall originate from morphogenetic events during the first/early second trimester. Here, we show that the temporal dynamics of $CB_1R$ expression is distinct in Down's syndrome: The appearance of $CB_1Rs$ is delayed, particularly during the early phase of brain development (first/second trimesters), and stays disproportionately high also at foetal periods when $CB_1R$ expression in controls becomes reduced. These pathogenic changes could provoke an imbalance of neurogenesis, radial cell migration [12] and morphogenesis leading to cortical delamination in Down's syndrome. We could not identify a morphological difference of $CB_1R^+$ profiles in Down's syndrome, supporting that the time factor, but not compartmentalization, is a principal determinant of altered endocannabinoid signalling.

Testing the distribution of $CB_1Rs$ does not equal the study of the entire endocannabinoid system, which includes enzymes, receptor-interacting proteins (like CRIP1a [65]) and putative transporters. Nevertheless, we are confident in our data because human neuropathology studies in congenital neurological and psychiatric conditions (e.g., epilepsy [66, 67], schizophrenia [68], fragile X syndrome [69] and attention-deficit spectrum disorder [70]) highlight that changes in $CB_1R$ distribution faithfully capture the involvement, as well as impairment of the endocannabinoid system in disease pathogenesis. Moreover, a recent study on temporal changes in the expression of $GABA_A$ receptor subunits in utero highlighted that temporal modifications of ionotropic receptor expression that directly gate synaptic neurotransmission are delayed in Down's syndrome [71]. This finding also linked foetal changes in synaptogenesis to excess β-amyloid load in Down's syndrome brains. Therefore, we suggest that altered $CB_1R$ expression might be both a surrogate for impaired neuronal migration/specification and causal to errant synaptic connectivity and plasticity in this devastating disorder.

We propose that Down's syndrome is associated with not only delayed $CB_1R$ expression but also increased $CB_1R$ responsiveness. This hypothesis is based on our in vitro neuropharmacology data from $Ts65Dn^{+/+}$ neurons, which were found to be more sensitive to $CB_1R$ stimulation than their wild-type counterparts. These findings are supported by data showing that $CB_1R$ expression and function are increased in the hippocampus of adult $Ts65Dn^{+/+}$ mice and its pharmacological inhibition restores synaptic plasticity, memory processes and neurogenesis [45]. The novelty of our study derives from showing that increased $CB_1R$ responsiveness persists throughout the lifetime of $Ts65Dn^{+/+}$ neurons, at least in vitro, and is due, at least in part, to the accelerated breakdown of SCG10/stathmin-2, a key component of the microtubule elongation and proofreading machinery in neurites [43]. Of note, reduced *Stmn2*/SCG10 mRNA expression was also reported in neurospheres derived from foetuses with Down's syndrome [42]. Indeed, an increased concentration of acetylated tubulin, a post-translational modification indicative of excess microtubule stability and slowed turnover (i.e., 'ageing') [52], is poised to link $CB_1R$ hypersensitivity-aberrant SCG10 degradation-increased tubulin stability-slowed brain development in foetuses with Down's syndrome [18].

Community-wide genotoxicity studies from the National Survey of Drug Use and Health (2003–2017) and the National Birth Defects Prevention Network demonstrated elevated rates of Down's syndrome in infants prenatally exposed to THC, cannabigerol and cannabichromene, and this association fulfilled formal quantitative criteria of causality [72]. Therefore, we suggest that maternal cannabinoid use during pregnancy could aggravate the genetic penetrance and clinical manifestation of Down's syndrome.

## AUTHOR CONTRIBUTIONS

A.A. and T.H. conceived the study. J.H., T.H., G.K. and A.A. designed the experiments. A.A. and T.H. procured the funding. A.P., J.H. and G.Z. performed the experiments and analysed the data. All authors contributed to writing the manuscript and approved its submitted version.

## ACKNOWLEDGEMENTS

We thank Dr. Erik Keimpema (Medical University of Vienna, Austria) for helpful discussions and Dr. Ken Mackie (Indiana University, USA) for his gift of the anti-$CB_1R$ antibody.

## CONFLICT OF INTEREST STATEMENT

The authors declare no conflict of interest. GK is an executive editor of *Neuropathology and Applied Neurobiology*. The Editors of *Neuropathology and Applied Neurobiology* are committed to peer-review integrity and upholding the highest standards of review. As such, this article was peer-reviewed by independent, anonymous expert referees, and the authors (including GK) had no role in either the editorial decision or the handling of the paper.

## DATA AVAILABILITY STATEMENT

The data that support the findings of this study are available from the corresponding author upon reasonable request.

## ETHICS STATEMENT

This study was performed according to the Declaration of Helsinki. Analysis was performed according to an approval for histopathology

by the Human Ethical Committee of the Medical University of Vienna (No. 104/2009).

## ORCID

*Gábor G. Kovács* https://orcid.org/0000-0003-3841-5511

## PEER REVIEW

The peer review history for this article is available at https://publons.com/publon/10.1111/nan.12887.

## REFERENCES


1. Alexandre J, Carmo H, Carvalho F, Silva JP. Synthetic cannabinoids and their impact on neurodevelopmental processes. *Addict Biol*. 2020;25(2):e12824. doi:10.1111/adb.12824
2. Alpar A, di Marzo V, Harkany T. At the tip of an iceberg: prenatal marijuana and its possible relation to neuropsychiatric outcome in the offspring. *Biol Psychiatry*. 2016;79(7):e33-e45. doi:10.1016/j.biopsych.2015.09.009
3. Harkany T, Guzman M, Galve-Roperh I, Berghuis P, Devi LA, Mackie K. The emerging functions of endocannabinoid signaling during CNS development. *Trends Pharmacol Sci*. 2007;28(2):83-92. doi:10.1016/j.tips.2006.12.004
4. Katona I, Sperlágh B, Maglóczky Z, et al. GABAergic interneurons are the targets of cannabinoid actions in the human hippocampus. *Neuroscience*. 2000;100(4):797-804. doi:10.1016/S0306-4522(00)00286-4
5. Katona I, Sperlágh B, Sík A, et al. Presynaptically located CB1 cannabinoid receptors regulate GABA release from axon terminals of specific hippocampal interneurons. *J Neurosci*. 1999;19(11):4544-4558. doi:10.1523/JNEUROSCI.19-11-04544.1999
6. Katona I, Urbán GM, Wallace M, et al. Molecular composition of the endocannabinoid system at glutamatergic synapses. *J Neurosci*. 2006;26(21):5628-5637. doi:10.1523/JNEUROSCI.0309-06.2006
7. Tanimura A, Yamazaki M, Hashimotodani Y, et al. The endocannabinoid 2-arachidonoylglycerol produced by diacylglycerol lipase alpha mediates retrograde suppression of synaptic transmission. *Neuron*. 2010;65(3):320-327. doi:10.1016/j.neuron.2010.01.021
8. Devane WA, Hanus L, Breuer A, et al. Isolation and structure of a brain constituent that binds to the cannabinoid receptor. *Science*. 1992;258(5090):1946-1949. doi:10.1126/science.1470919
9. Walker DJ, Suetterlin P, Reisenberg M, Williams G, Doherty P. Down-regulation of diacylglycerol lipase-alpha during neural stem cell differentiation: identification of elements that regulate transcription. *J Neurosci Res*. 2010;88(4):735-745. doi:10.1002/jnr.22251
10. Diaz-Alonso J, Guzman M, Galve-Roperh I. Endocannabinoids via CB(1) receptors act as neurogenic niche cues during cortical development. *Philos Trans R Soc Lond B Biol Sci*. 2012;367(1607):3229-3241. doi:10.1098/rstb.2011.0385
11. Galve-Roperh I, Chiurchiu V, Diaz-Alonso J, Bari M, Guzman M, Maccarrone M. Cannabinoid receptor signaling in progenitor/stem cell proliferation and differentiation. *Prog Lipid Res*. 2013;52(4):633-650. doi:10.1016/j.plipres.2013.05.004
12. Morozov YM, Mackie K, Rakic P. Cannabinoid type 1 receptor is undetectable in rodent and primate cerebral neural stem cells but participates in radial neuronal migration. *Int J Mol Sci*. 2020;21(22):8657. doi:10.3390/ijms21228657
13. Begbie J, Doherty P, Graham A. Cannabinoid receptor, CB1, expression follows neuronal differentiation in the early chick embryo. *J Anat*. 2004;205(3):213-218. doi:10.1111/j.0021-8782.2004.00325.x
14. Mulder J, Aguado T, Keimpema E, et al. Endocannabinoid signaling controls pyramidal cell specification and long-range axon patterning. *Proc Natl Acad Sci U S a*. 2008;105(25):8760-8765. doi:10.1073/pnas.0803545105
15. Sonego M, Gajendra S, Parsons M, et al. Fascin regulates the migration of subventricular zone-derived neuroblasts in the postnatal brain. *J Neurosci*. 2013;33(30):12171-12185. doi:10.1523/JNEUROSCI.0653-13.2013
16. Keimpema E, Barabas K, Morozov YM, et al. Differential subcellular recruitment of monoacylglycerol lipase generates spatial specificity of 2-arachidonoyl glycerol signaling during axonal pathfinding. *J Neurosci*. 2010;30(42):13992-14007. doi:10.1523/JNEUROSCI.2126-10.2010
17. Keimpema E, Alpar A, Howell F, et al. Diacylglycerol lipase alpha manipulation reveals developmental roles for intercellular endocannabinoid signaling. *Sci Rep*. 2013;3(1):2093. doi:10.1038/srep02093
18. Tortoriello G, Morris CV, Alpár A, et al. Miswiring the brain: Δ9-tetrahydrocannabinol disrupts cortical development by inducing an SCG10/stathmin-2 degradation pathway. *EMBO j*. 2014;33(7):668-685. doi:10.1002/embj.201386035
19. Alpár A, Tortoriello G, Calvigioni D, et al. Endocannabinoids modulate cortical development by configuring Slit2/Robo1 signalling. *Nat Commun*. 2014;5:54421. doi:10.1038/ncomms5421
20. Albarran E, Sun Y, Liu Y, et al. Postsynaptic synucleins mediate vesicular exocytosis of endocannabinoids. *bioRxiv*. 2021;2021. doi:10.1101/2021.10.04.462870
21. Maccarrone M, Guzman M, Mackie K, Doherty P, Harkany T. Programming of neural cells by (endo)cannabinoids: from physiological rules to emerging therapies. *Nat Rev Neurosci*. 2014;15(12):786-801. doi:10.1038/nrn3846
22. Estrada JA, Contreras I. Endocannabinoid receptors in the CNS: potential drug targets for the prevention and treatment of neurologic and psychiatric disorders. *Curr Neuropharmacol*. 2020;18(8):769-787. doi:10.2174/1570159X18666200217140255
23. Herkenham M, Lynn AB, Little MD, et al. Cannabinoid receptor localization in brain. *Proc Natl Acad Sci U S a*. 1990;87(5):1932-1936. doi:10.1073/pnas.87.5.1932
24. Berghuis P, Rajnicek AM, Morozov YM, et al. Hardwiring the brain: endocannabinoids shape neuronal connectivity. *Science*. 2007;316(5828):1212-1216. doi:10.1126/science.1137406
25. Bernard C, Milh M, Morozov YM, Ben-Ari Y, Freund TF, Gozlan H. Altering cannabinoid signaling during development disrupts neuronal activity. *Proc Natl Acad Sci U S a*. 2005;102(26):9388-9393. doi:10.1073/pnas.0409641102
26. Morozov YM, Freund TF. Post-natal development of type 1 cannabinoid receptor immunoreactivity in the rat hippocampus. *Eur J Neurosci*. 2003;18(5):1213-1222. doi:10.1046/j.1460-9568.2003.02852.x
27. Alger BE. Retrograde signaling in the regulation of synaptic transmission: focus on endocannabinoids. *Prog Neurobiol*. 2002;68(4):247-286. doi:10.1016/S0301-0082(02)00080-1
28. Monory K, Polack M, Remus A, Lutz B, Korte M. Cannabinoid CB1 receptor calibrates excitatory synaptic balance in the mouse hippocampus. *J Neurosci*. 2015;35(9):3842-3850. doi:10.1523/JNEUROSCI.3167-14.2015
29. Diaz-Alonso J, Aguado T, Wu CS, et al. The CB(1) cannabinoid receptor drives corticospinal motor neuron differentiation through the Ctip2/Satb2 transcriptional regulation axis. *J Neurosci*. 2012;32(47):16651-16665. doi:10.1523/JNEUROSCI.0681-12.2012
30. Bromberg KD, Ma'ayan A, Neves SR, Iyengar R. Design logic of a cannabinoid receptor signaling network that triggers neurite outgrowth. *Science*. 2008;320(5878):903-909. doi:10.1126/science.1152662
31. Calvigioni D, Hurd YL, Harkany T, Keimpema E. Neuronal substrates and functional consequences of prenatal cannabis exposure. *Eur Child Adolesc Psychiatry*. 2014;23(10):931-941. doi:10.1007/s00787-014-0550-y

32. Nardou R, Ferrari DC, Ben-Ari Y. Mechanisms and effects of seizures in the immature brain. *Semin Fetal Neonatal Med*. 2013;18(4):175-184. doi:10.1016/j.siny.2013.02.003
33. Scheyer AF, Melis M, Trezza V, Manzoni OJJ. Consequences of perinatal cannabis exposure. *Trends Neurosci*. 2019;42(12):871-884. doi:10.1016/j.tins.2019.08.010
34. Neuhofer D, Henstridge CM, Dudok B, et al. Functional and structural deficits at accumbens synapses in a mouse model of fragile X. *Front Cell Neurosci*. 2015;9:100. doi:10.3389/fncel.2015.00100
35. Soltesz I, Alger BE, Kano M, et al. Weeding out bad waves: towards selective cannabinoid circuit control in epilepsy. *Nat Rev Neurosci*. 2015;16(5):264-277. doi:10.1038/nrn3937
36. Heussler H, Cohen J, Silove N, et al. A phase 1/2, open-label assessment of the safety, tolerability, and efficacy of transdermal cannabidiol (ZYN002) for the treatment of pediatric fragile X syndrome. *J Neurodev Disord*. 2019;11(1):16. doi:10.1186/s11689-019-9277-x
37. Gomis-Gonzalez M, Busquets-Garcia A, Matute C, Maldonado R, Mato S, Ozaita A. Possible therapeutic doses of cannabinoid type 1 receptor antagonist reverses key alterations in fragile X syndrome mouse model. *Genes (Basel)*. 2016;7(9). doi:10.3390/genes7090056
38. Dierssen M. Down syndrome: the brain in trisomic mode. *Nat Rev Neurosci*. 2012;13(12):844-858. doi:10.1038/nrn3314
39. Altuna M, Gimenez S, Fortea J. Epilepsy in down syndrome: a highly prevalent comorbidity. *J Clin Med*. 2021;10(13):2776. doi:10.3390/jcm10132776
40. Ross MH, Galaburda AM, Kemper TL. Down's syndrome: is there a decreased population of neurons? *Neurology*. 1984;34(7):909-916. doi:10.1212/wnl.34.7.909
41. Golden JA, Hyman BT. Development of the superior temporal neocortex is anomalous in trisomy 21. *J Neuropathol Exp Neurol*. 1994;53(5):513-520. doi:10.1097/00005072-199409000-00011
42. Bahn S, Mimmack M, Ryan M, et al. Neuronal target genes of the neuron-restrictive silencer factor in neurospheres derived from fetuses with Down's syndrome: a gene expression study. *Lancet*. 2002;359(9303):310-315. doi:10.1016/S0140-6736(02)07497-4
43. Riederer BM, Pellier V, Antonsson B, et al. Regulation of microtubule dynamics by the neuronal growth-associated protein SCG10. *Proc Natl Acad Sci U S a*. 1997;94(2):741-745. doi:10.1073/pnas.94.2.741
44. Reeves RH, Irving NG, Moran TH, et al. A mouse model for Down syndrome exhibits learning and behaviour deficits. *Nat Genet*. 1995;11(2):177-184. doi:10.1038/ng1095-177
45. Navarro-Romero A, Vazquez-Oliver A, Gomis-Gonzalez M, et al. Cannabinoid type-1 receptor blockade restores neurological phenotypes in two models for Down syndrome. *Neurobiol Dis*. 2019;125:92-106. doi:10.1016/j.nbd.2019.01.014
46. Aziz NM, Guedj F, Pennings JLA, et al. Lifespan analysis of brain development, gene expression and behavioral phenotypes in the Ts1Cje, Ts65Dn and Dp(16)1/Yey mouse models of Down syndrome. *Dis Model Mech*. 2018;11(6). doi:10.1242/dmm.031013
47. Diaz-Alonso J, de Salas-Quiroga A, Paraiso-Luna J, et al. Loss of cannabinoid CB1 receptors induces cortical migration malformations and increases seizure susceptibility. *Cereb Cortex*. 2017;27(11):5303-5317. doi:10.1093/cercor/bhw309
48. Pinter A, Hevesi Z, Zahola P, Alpar A, Hanics J. Chondroitin sulfate proteoglycan-5 forms perisynaptic matrix assemblies in the adult rat cortex. *Cell Signal*. 2020;74:109710. doi:10.1016/j.cellsig.2020.109710
49. Keimpema E, Tortoriello G, Alpar A, et al. Nerve growth factor scales endocannabinoid signaling by regulating monoacylglycerol lipase turnover in developing cholinergic neurons. *Proc Natl Acad Sci U S A*. 2013;110(5):1935-1940. doi:10.1073/pnas.1212563110
50. Bradford MM. A rapid and sensitive method for the quantitation of microgram quantities of protein utilizing the principle of protein-dye binding. *Anal Biochem*. 1976;(72):248-254. doi:10.1016/0003-2697(76)90527-3
51. Fuzik J, Rehman S, Girach F, et al. Brain-wide genetic mapping identifies the indusium griseum as a prenatal target of pharmacologically unrelated psychostimulants. *Proc Natl Acad Sci U S a*. 2019;116(51):25958-25967. doi:10.1073/pnas.1904006116
52. Maruta H, Greer K, Rosenbaum JL. The acetylation of alpha-tubulin and its relationship to the assembly and disassembly of microtubules. *J Cell Biol*. 1986;103(2):571-579. doi:10.1083/jcb.103.2.571
53. Jordan JD, He JC, Eungdamrong NJ, et al. Cannabinoid receptor-induced neurite outgrowth is mediated by Rap1 activation through G (alpha)o/i-triggered proteasomal degradation of Rap1GAPII. *J Biol Chem*. 2005;280(12):11413-11421. doi:10.1074/jbc.M411521200
54. He JC, Gomes I, Nguyen T, et al. The G alpha(o/i)-coupled cannabinoid receptor-mediated neurite outgrowth involves Rap regulation of Src and Stat3. *J Biol Chem*. 2005;280(39):33426-33434. doi:10.1074/jbc.M502812200
55. Wang X, Dow-Edwards D, Keller E, Hurd YL. Preferential limbic expression of the cannabinoid receptor mRNA in the human fetal brain. *Neuroscience*. 2003;118(3):681-694. doi:10.1016/S0306-4522(03)00020-4
56. Mato S, del Olmo E, Pazos A. Ontogenetic development of cannabinoid receptor expression and signal transduction functionality in the human brain. *Eur J Neurosci*. 2003;17(9):1747-1754. doi:10.1046/j.1460-9568.2003.02599.x
57. Oudin MJ, Gajendra S, Williams G, Hobbs C, Lalli G, Doherty P. Endocannabinoids regulate the migration of subventricular zone-derived neuroblasts in the postnatal brain. *J Neurosci*. 2011;31(11):4000-4011. doi:10.1523/JNEUROSCI.5483-10.2011
58. Vitalis T, Laine J, Simon A, Roland A, Leterrier C, Lenkei Z. The type 1 cannabinoid receptor is highly expressed in embryonic cortical projection neurons and negatively regulates neurite growth in vitro. *Eur J Neurosci*. 2008;28(9):1705-1718. doi:10.1111/j.1460-9568.2008.06484.x
59. Keimpema E, di Marzo V, Harkany T. Biological basis of cannabinoid medicines. *Science*. 2021;374(6574):1449-1450. doi:10.1126/science.abf6099
60. Molnar Z, Clowry GJ, Sestan N, et al. New insights into the development of the human cerebral cortex. *J Anat*. 2019;235(3):432-451. doi:10.1111/joa.13055
61. Contestabile A, Fila T, Ceccarelli C, et al. Cell cycle alteration and decreased cell proliferation in the hippocampal dentate gyrus and in the neocortical germinal matrix of fetuses with Down syndrome and in Ts65Dn mice. *Hippocampus*. 2007;17(8):665-678. doi:10.1002/hipo.20308
62. Larsen KB, Laursen H, Graem N, Samuelsen GB, Bogdanovic N, Pakkenberg B. Reduced cell number in the neocortical part of the human fetal brain in Down syndrome. *Ann Anat*. 2008;190(5):421-427. doi:10.1016/j.aanat.2008.05.007
63. Stagni F, Giacomini A, Emili M, et al. Subicular hypotrophy in fetuses with Down syndrome and in the Ts65Dn model of Down syndrome. *Brain Pathol*. 2019;29(3):366-379. doi:10.1111/bpa.12663
64. Weitzdoerfer R, Dierssen M, Fountoulakis M, Lubec G. Fetal life in Down syndrome starts with normal neuronal density but impaired dendritic spines and synaptosomal structure. *J Neural Transm Suppl*. 2001;61(61):59-70. doi:10.1007/978-3-7091-6262-0_5
65. Guggenhuber S, Alpar A, Chen R, et al. Cannabinoid receptor-interacting protein Crip1a modulates CB1 receptor signaling in mouse hippocampus. *Brain Struct Funct*. 2016;221(4):2061-2074. doi:10.1007/s00429-015-1027-6
66. Katona I, Freund TF. Endocannabinoid signaling as a synaptic circuit breaker in neurological disease. *Nat Med*. 2008;14(9):923-930. doi:10.1038/nm.f.1869
67. Ludányi A, Erőss L, Czirják S, et al. Downregulation of the CB1 cannabinoid receptor and related molecular elements of the endocannabinoid system in epileptic human hippocampus. *J Neurosci*. 2008;28(12):2976-2990. doi:10.1523/JNEUROSCI.4465-07.2008

68. Murray RM, Englund A, Abi-Dargham A, et al. Cannabis-associated psychosis: neural substrate and clinical impact. *Neuropharmacology*. 2017;124:89-104. doi:10.1016/j.neuropharm.2017.06.018
69. Martin BS, Huntsman MM. Pathological plasticity in fragile X syndrome. *Neural Plast*. 2012;2012:275630. doi:10.1155/2012/275630
70. de Pol M, Kolla NJ. Endocannabinoid markers in autism spectrum disorder: a scoping review of human studies. *Psychiatry Res*. 2021;306:114256. doi:10.1016/j.psychres.2021.114256
71. Milenkovic I, Stojanovic T, Aronica E, et al. GABAA receptor subunit deregulation in the hippocampus of human foetuses with Down syndrome. *Brain Struct Funct*. 2018;223(3):1501-1518. doi:10.1007/s00429-017-1563-3
72. Reece AS, Hulse GK. Epidemiological overview of multidimensional chromosomal and genome toxicity of cannabis exposure in congenital anomalies and cancer development. *Sci Rep*. 2021;11(1):13892. doi:10.1038/s41598-021-93411-5


## SUPPORTING INFORMATION

Additional supporting information can be found online in the Supporting Information section at the end of this article.

**How to cite this article:** Patthy Á, Hanics J, Zachar G, Kovács GG, Harkany T, Alpár A. Regional redistribution of CB1 cannabinoid receptors in human foetal brains with Down's syndrome and their functional modifications in Ts65Dn$^{+/+}$ mice. *Neuropathol Appl Neurobiol*. 2023;49(1):e12887. doi:10.1111/nan.12887